# Power balance for impurity seeded ergodic divertor discharges in Tore Supra

R. Reichle, J.C. Vallet, V. Basiuk, M. Chantant, R. Giannella, R. Guirlet, R. Mitteau

*Association EURATOM-CEA sur la fusion,*
*C.E.-Cadarache, 13108 St. Paul-lez-Durance, France*

## 1. Introduction

To minimise the power load on target plates via radiation losses is crucial for any next step device. Tore Supra (TS) investigates as alternative to axisymmetric divertors, the radiative properties of the Ergodic Divertor (ED). It has been postulated on the basis of a power-balance method [1] that the total radiation can be 1.5 times higher than the actual bolometer [2] measurements due to local radiation enhancement near the target plates, outside the lines of sight of the bolometer array. For detachment this factor is 1. The relevance of this factor is that 1 corresponds to an agreement with the multi-machine scaling law for radiation [3]. The ripple losses were deemed to amount to 30% of the ICRH energy. Improvements in the analysis of the calorimetry indicate that for ohmic discharges 100% of the input energy are recovered, whereas 30% of the ICRH heating power are missing [4], which seems to confirm the power balance finding. The main emphasis of the present contribution is the search for independent indications concerning local radiation enhancement in the vicinity of target plates by the application of the power-balance analyis to impurity seeded discharges and the use of spatially resolved calorimetry.

## 2. Measurements

Fig. 1 shows an ICRH heated discharge with Argon puffing. The radiation $P_{radhor}$ as measured by the horizontal bolometer array and $T_{div}$, the temperature rise of the $B_4C$ surface of the target plates of the ergodic divertor [5] react strongly on the impurity gas puff. The $P_{radhor}$ trace is more positively peaked in time than the $T_{div}$ trace is negatively peaked around the time of the maximum of the Argon trace. $I_{rip}$, the ion current caused by lost ripple particles [6] is positively correlated to ICRH heating power $P_{ICRH}$ and inversely to the electron density $n_e$. Fig. 2 shows the spatial distribution of the energy outflux determined by calorimetry. The limiter receives higher flux densities 3than the ergodic divertor target plates.
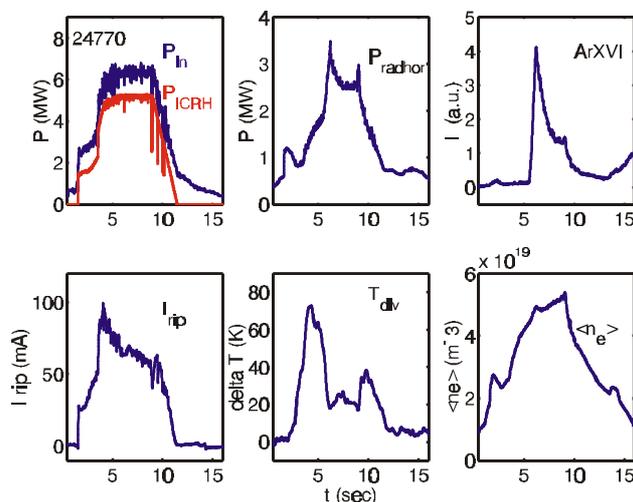


*Fig. 1: Typical discharge traces for an impurity seeded ICRH heated ED discharge. $P_{in}$ is the total input power, $P_{ICRH}$ the ICRH heating power, $P_{radhor}$ the estimate of the total radiation from the horizontal bolometer array, ArXVI is a spectral line of argon (353.6 Å), $I_{rip}$ the current measurement of the ripple trapped ions, $T_{div}$ the average temperature rise on the divertor target plates, $n_e$ the electron density.*
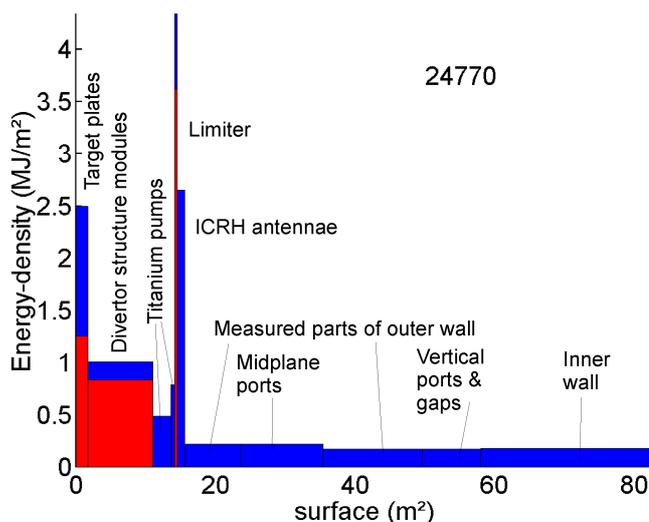
*Fig. 2.: Spatial distribution of energy deposition according to calorimetry. From left to right: ED target plates, ED structure, normal titanium pumps, titanium pumps next to limiter, limiter (maximum 20.8 MJ/m$^2$ ), ICRH antennae, outer wall midplane, midplane ports, rest of outer wall, vertical ports, inner wall. In red: localised extra radiation as extrapolated from the titanium pump measurements.*

The interesting point are the fluxes falling onto the titanium pumps at the side of these target objects (see fig. 3). All of them receive higher flux densities than the outer wall. The pump next to the limiter receives a significantly higher flux than the ones only adjacent to a divertor. The energy flux on the inner wall is found to be practically equal to the energy flux on the outer wall.

## 3. Analysis

Four analysis methods have been employed. The first method uses the measurements of $P_{radhor}$, $T_{div}$ and $I_{rip}$ and adjusts individual fitparameters $F_{rad}$, $F_{dep}$ and $F_{rip}$ such that $P_{balance}=P_{in}-P_{rad}-P_{de}-P_{loss}$- dW/dt is minimised, where $P_{in}$ is the total input power, $P_{rad}=F_{rad} \cdot P_{radhor}$ the total radiation, $P_{dep}=T_{div} \cdot F_{dep}$ [1,5] the total conducted power and $P_{loss}=I_{rip} \cdot F_{rip}$ the lost power not used for heating the plasma.

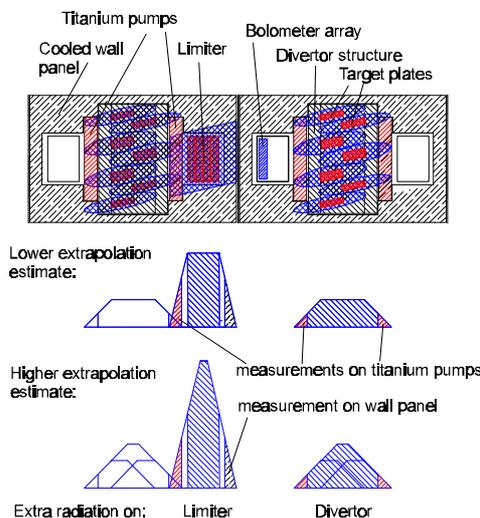The second method is to use the enhancement of the



*Fig. 3: Geometry of outer wall with ED, titanium pumps, limiter, horizontal bolometer sight lines. Superimposed is the assumed extra radiation distributions. Below projections of an upper and a lower extrapolation estimate of the presumed extra-radiation deposition onto the outer wall for both the ED and the limiter.*

flux on the titanium pumps (see fig. 2) to estimate $E_{rad}$ the integral of $P_{rad}$. Based on the simplified assumption that the extra radiation near a target falls off linearly over 40 cm in the parallel direction and 15 cm in the perpendicular direction (fig. 3) the total local extra

radiation created in the vicinity of the limiter and directed towards the outer wall, is estimated to be about 11.5 (± 2.5) times as much as the extra radiation on the adjacent titanium pump when compared with the load on the other titanium pumps. The part of the extra radiation which falls onto the limiter itself is 67% of this radiation. What can be seen as justification to the assumption of the 40 cm fall off length is that the enhancements from the limiter are only measurable on the nearby titanium pump and the nearby wall panel. The effect on the adjacent bolometer is much smaller. It is only ≈ 10% of the enhancement on the titanium pump next to the limiter. Similarly the total extra radiation on the divertor is estimated to be 12 (±1.3) times larger than the extra radiation on the titanium pumps when taking the load on the standard

Fig. 4: Illustration of the power balance method. Best results are achieved when assuming that $F_{rad}$ is lowered when heavy impurities are puffed and then stepped down to 1 when the discharge detaches.

outer wall panels as reference. Even though the $D_\alpha$ distribution is very peaked at the protruding tip at one end of the divertor target plates, the CIII emission falls off only slightly in the parallel flux direction along the plates, and less than a factor 2 over 10 cm perpendicular to them. This is also seen as being compatible with the assumed fall off lengths of the localised extra-radiation. The total of $E_{rad}$ is for this analysis calculated as the sum of these extrapolated extra radiations (illustrated in fig. 2) plus the calorimetry measurements on inner and outer wall, extrapolated for the uncovered port areas. Part of the localised extra radiation should fall onto the inner wall.

Based on tomographic reconstructions for ED discharges [2,4] and an extrapolation factor of the surface one can estimate that the total radiation should be 5.1 times larger 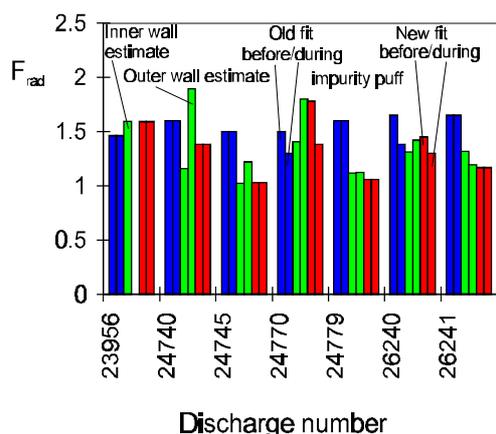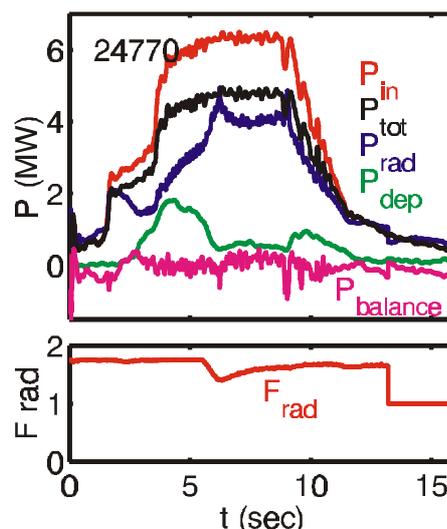than the calorimetric measurement from the inner wall. The ratio between this estimate and the radiation measured by the bolometer is the simplest estimate (third method) of the enhancement factor $F_{rad}$.

The fourth method, which is an improved multi-parameter fit method is to determine first the energy loss by calorimetry as a fraction $F_{ICRH}$ of the ICRH-energy and then to fit $T_{div}$ and $P_{rad}$ to a remaining total power $P_{tot}=Pin-F_{ICRH}\cdot P_{ICRH}$. In the case of heavy impurity injection it is furthermore proposed to make $F_{rad}$ a function of the impurity radiation intensity $I_{imp}$ such that $F_{rad}(t) = F_{radmax}-C\cdot I_{imp}(t)/P_{radhor}(t)$, where C is also fitted. An illustration of this procedure is given in fig.4 where $P_{loss}$ is 30% of the ICRH-power and the variation of $F_{rad}$ is between 1.78 and 1.38. The results of the different methods

Fig. 5: Estimates of $F_{rad}$: the normal fit procedure (blue), the estimate based on the inner wall calorimetry (1st green), outer wall estimate (2nd green), improved fit (red). For the fits: The left value is before and the right value is during the impurity injection. (24770 Ar, 26240 Ne).

concerning the postulated radiation asymmetry are summarised in fig. 5 which shows the resulting $F_{rad}$ factors for discharges with and without impurity seeding. Both calorimetric values and the advanced fitting procedure assuming 30% ICRH losses agree rather well. The original fitting procedure is less precise and gives slightly higher $F_{rad}$ values. The trend that the injection of heavy impurities lowers $F_{rad}$ is seen with both fitting procedures. The other clear trend is, that $F_{rad}$ falls with rising density, getting close to unity near detachment (fig. 6). The discharges with Neon or Argon are distinct from the trend of the discharges with intrinsic impurities.

## 4. Discussion and conclusions



*Fig. 6: $F_{rad}$ values against the electron density for the discharges of fig 5. The red values are the results of the improved fit procedure. The blue ones are the average of the two calorimetric procedures. The dots and crosses are intrinsic impurities. The triangles are Argon, the squares Neon. The open symbols are the initial values of $F_{rad}$ before the impurity is puffed*

All methods confirm the existence of an important local radiation enhancement in front of target objects. Their toroidally localised nature and the lack of short scale toroidal resolution of the bolometers cause an underestimate of the radiation. Observed corrective factors for radiative divertor discharges range between 1.1 and 1.6 depending on the density. The impurity seeded discharges show during the impurity injection a reduction of this factor which can be explained by the radiation distribution becoming toroidally more symmetric due to the larger ionisation lengths. The consistency of the results (fig. 6) seems to validate the assumption of a fall off length of the radiation of 40 cm as used for the radiation extrapolation from the outboard calorimetry. The localised extra radiation falling onto one individual neutraliser is about 1 kW (fig. 2). This should be compared with spectroscopic radiation measurements and modelling [7] to see whether there is room for charge exchange neutrals to be important. The fact, that there is a strong dependency on density seems to indicate, that neutrals may play an important role. With the observed loss fraction of 30% of the ICRH and the deposition profiles on the ripple detector [6] one can estimate an upper limit for the extra heat load onto the planned toroidal limiter, the next upgrade of Tore Supra kown as CIEL, to be maximal 2.3±0.9 MW/m$^2$ in the central area between adjacent toroidal field coils for an RF heating power of 10 MW. It is however difficult at the present stage to decide how much of the losses detected as deficit in the calorimetry have to be attributed to the ripple losses and how much to an overestimate of the ICRH power coupled. The observation, that a fit using the measured ripple current as proportional to the losses, overestimates $F_{rad}$ slightly (fig.5), whereas a fit using the ICRH power seems to underestimate $F_{rad}$ slightly (fig. 6) in comparison with the calorimetric values, seems to indicate that both effects have to be considered.

[1] Reichle, R., et al., Contr. 25$^{th}$ EPS,, 29 June - 3 July 1998, Praha, Czech Republic.
[2] Vallet, J.C, et al., Contr. 24$^{th}$ EPS, 9 - 13 June 1997, Berchtesgaden, Germany
[3] Matthews, G.F., et al., Nucl. Fusion 39 (1999) 19.
[4] Vallet, J.C., et al., this conference.
[5] Grosman, A., et al., JNM 241-243 (1997) 532-537.
[6] Basiuk, V., et al., Nucl. Fus., Vol 35, No 12 (1995) 1593-1596.
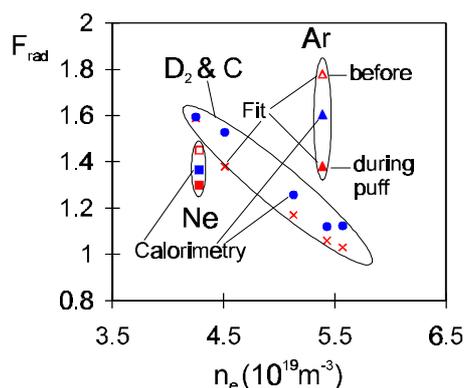[7] Giannella, R., et al., this conference.